THE JOURNAL OF BIOLOGICAL CHEMISTRY VOL. 286, NO. 47, pp. 40631–40637, November 25, 2011

Molecular Convergence of Bacterial and Eukaryotic Surface Order*

Received for publication, June 28, 2011, and in revised form, September 20, 2011 Published, JBC Papers in Press, September 30, 2011, DOI 10.1074/jbc.M111.276444

Hermann-Josef Kaiser[‡], Michal A. Surma[‡], Florian Mayer[§], Ilya Levental[‡], Michal Grzybek[‡], Robin W. Klemm[¶], Sandrine Da Cruz[‖], Chris Meisinger[‡‡], Volker Müller[§], Kai Simons[‡], and Daniel Lingwood[‡1]**

From the [‡]Max Planck Institute for Molecular Cell Biology and Genetics, Pfotenhauerstrasse 108, Dresden 01307, Germany, the [§]Department of Molecular Microbiology & Bioenergetics, Institute of Molecular Biosciences, Goethe-Universität Frankfurt, Max-von-Laue-Strasse 9, Frankfurt am Main 60438, Germany, the [¶]Department of Cell Biology, Harvard Medical School, Boston, Massachusetts 02115, the [‖]Ludwig Institute and Department of Cellular and Molecular Medicine, University of California at San Diego, La Jolla, California 92093-0670, the [**]Institut für Biochemie und Molekularbiologie, Zentrum für Biochemie und Molekulare Zellforschung (ZBMZ), Universität Freiburg, Freiburg D-79104, Germany, and the [‡‡]Centre for Biological Signaling Studies (BIOSS), Universität Freiburg, Freiburg 79104, Germany

Background: Living cells maintain a fluid membrane at their surface.
Results: Bacteria and eukaryotes display comparable surface order. Transmembrane proteins order cell membranes in the absence of sterol (Bacteria) and disorder in its presence (Eukarya).
Conclusion: Bidirectional ordering may provide a means to achieve similar barrier properties despite compositional differences.
Significance: Nature may use different protein/lipid combinations to standardize cell surface order.

The conservation of fluidity is a theme common to all cell membranes. In this study, an analysis of lipid packing was conducted via C-laurdan spectroscopy of cell surface membranes prepared from representative species of *Bacteria* and *Eukarya*. We found that despite their radical differences in composition (namely the presence and absence of membrane-rigidifying sterol) the membrane order of all taxa converges on a remarkably similar level. To understand how this similarity is constructed, we reconstituted membranes with either bacterial or eukaryotic components. We found that transmembrane segments of proteins have an important role in buffering lipid-mediated packing. This buffering ensures that sterol-free and sterol-containing membranes exhibit similar barrier properties.

Cell membranes are among the few structures in biology that are not shaped by the intrinsic attraction of their molecular building blocks. Instead, the bilayer composite arises through the hydrophobic effect, wherein lipids and hydrophobic proteins are excluded from the dense hydrogen-bonding network of the surrounding water (1). This means of assembly engenders the membrane with crucial fluidity, allowing for shape flexibility as well as functional dynamics. However, as a hydrophobic layer alone does not equate to the capacity to encapsulate life, the importance of understanding the additional cell membrane-building specificities becomes apparent (2). Here its function as a selectively permeable barrier requires mechanical and chemical robustness, *i.e.* rigidity to resist rupture and leakage. Such tightening can be achieved by increasing the molecular packing in the hydrophobic core of the membrane (3, 4). Regulation of lipid composition is one means to influence packing and thereby balance rigidity and fluidity (5, 6). However, despite the increasing understanding of the physicochemical properties of model membranes (7–9), structural studies of cell membranes have begun to identify clear discrepancies between the model and the cell (10, 11). Here integral membrane proteins account for one-third of the proteome (12), meaning that, unlike model systems, cell membranes, both eukaryotic and bacterial, are most appropriately understood as lipid-protein composites in which membrane protein occupies a substantial surface area (13, 14). This large protein content has been proposed to influence many physiochemical properties of the membrane such as bilayer thickness (10), translational diffusivity (15), and membrane heterogeneity (11, 16), leaving us with the question of how to properly define lipid-protein architecture at the cell surface.

To gain more insight into the structure of cell membranes, we focused on membrane order, a parameter encompassing conformational packing of bilayer constituents (17). We began by measuring this parameter in surface membranes purified from a number of species representing members of the eukaryotic and bacterial domains of life. Surface membrane was defined as the cell membrane directly encapsulating the cytosol. We found that, despite their lack of membrane-rigidifying cholesterol, bacterial membranes exhibited a strikingly similar level of order as their eukaryotic counterparts. Membrane protein was identified as the basis for this convergence. Our data suggest that lipids and proteins act synergistically in the absence of sterol and

* This work was supported by a Max Planck Institute for Molecular Cell Biology and Genetics stipend (to D. L.), by Deutsche Forschungsgemeinschaft (DFG) Sonderforschungsbereiche Grant 807 (to V. M.), and by DFG Schwerpunktprogramm1175 Grant SI459/2-1, DFG Transregio 83 Grant TRR83 TP02; European Science Foundation LIPIDPROD Grant SI459/3-1; Bundesministerium für Bildung und Forschung ForMaT Grant 03FO1212, and The Klaus Tschira Foundation (to K. S.).
[1] To whom correspondence should be addressed: Vaccine Research Center, NIAID, National Institutes of Health, Bethesda, MD 20892-3005. E-mail: daniel.lingwood@nih.gov.

antagonistically in its presence. This translates to a bifunctional capacity by which membrane proteins may tune robustness and strength at the cell surface.

EXPERIMENTAL PROCEDURES

Reagents—Unless otherwise stated, all reagents were from Sigma. POPC,[2] POPG, POPE, SM (d18:1/C18:0), and cholesterol were purchased from Avanti Polar Lipids (Alabaster, AL). DDM was obtained from Glycon Biochemicals (Luckenwalds, Germany). For membrane reconstitution experiments, a synthetic transmembrane (TM) peptide (sequence = KKW-WLLLLLLLALLLLLLWWKK; a poly-leucine-hydrophobic peptide with tryptophans at the water-bilayer boundary and flanking lysines that readily form stable TM helices when reconstituted from organic solvent into bilayers (18–20)) was ordered from Genscript (Piscataway, NJ). The peptide was obtained at 98% purity, and stocks were prepared in ethanol. C-laurdan was a gift from Prof. B. R. Cho (Seoul, Korea). All stock concentrations of dyes were measured by spectroscopy, and all lipid stocks were measured by phosphate assay (Invitrogen).

Surface Membrane Preparation—Surface membranes were defined as the limiting cell barrier responsible for encapsulation of the cytosol. This organelle was prepared from both eukaryotic and bacterial cells according to published procedures (supplemental Methods and supplemental Figs. S1 and S2). For bacteria, surface membranes were obtained from Gram-negative (*Escherichia coli* inner membrane), Gram-positive (*Acetobacterium woodii* and *Bacillus subtilis*), and cyanobacteria (*Synechococcus* sp.) species. The eukaryotic counterparts included plasma membranes prepared from yeast (*Saccharomyces cerevisiae* and *Schizosaccharomyes pombe*), plants (*Lactuca sativa*), and mammalian sources (red blood cells (*Homo sapiens*), Rat basophil leukaemia (RBL) cells (*Rattus norvegicus*)). Eukaryotic internal membrane preparations served as non-surface membrane controls: endoplasmic reticulum, mitochondrial outer membrane, and mitochondrial inner membrane (supplemental Figs. S3 and S4).

Liposome/Proteoliposome Composition and Preparation—To scale the order of cell membranes, samples were compared with the extrema of liquid ordering in model membranes (11): liposomes of pure liquid ordered (Lo) phase (SM/cholesterol, molar ratio 1:1) and liposomes of pure liquid disordered (Ld) phase (POPC). To reconstitute protein/lipid specificity of bacteria, vesicles were assembled with bacterial inner membrane lipids (21) with or without TM peptide: POPG; POPG/POPE (molar ratio 1:1); POPG + 3 mol% TM peptide; POPG/POPE (molar ratio 1:1) + 3 mol% TM peptide. Eukaryotic lipid/protein specificity was reconstituted with plasma membrane lipids (22) with or without TM peptide: POPC; POPC/cholesterol (molar ratio 2:1); POPC/cholesterol/SM (molar ratio 1:1:1); POPC/cholesterol (molar ratio 2:1) + 3 mol% TM peptide; POPC/cholesterol/SM (molar ratio 1:1:1) + 3 mol% TM peptide. To assess the contribution of lipid *versus* protein in the cell surface membranes themselves, *E. coli* inner membrane and RBC plasma membranes were extracted for total lipids according to the two-step extraction procedure recently established for quantitative lipidomics (22–24) and formed into protein-free liposomes as described below.

For each composition, large unilamellar vesicles were prepared according to Kalvodova *et al.* (25), and proteoliposomes were formed by organic solvent reconstitution as described previously (11). Lipid or lipid/peptide mixtures were adjusted to the appropriate composition, evaporated under nitrogen, and then left under vacuum for 1 h. The dry film was then rehydrated in large unilamellar vesicles buffer (50 mM HEPES/150 mM NaCl, pH 7.4) and shaken for 40 min, all the time being heated above the T_m of the lipid mixture. The resulting homogeneous suspension was subjected to ten freeze-thaw cycles and then extruded through 100 nm pore diameter polycarbonate membrane using the Avanti mini-extruder. For proteoliposomes, TM peptide insertion was confirmed using a proteinase protection assay. Here, 10 μl of a 100 μg/ml large unilamellar vesicle suspension was incubated with proteinase K at 100 μg/ml in the presence or absence 0.5% SDS (w/v) and 0.5% Triton X-100 (w/v) for 3 h at 37 °C. Then PMSF was added to 100 mM. One volume of ethanol was added, and the sample was immediately heated for 2 min at 98 °C. The whole sample was applied to a silica TLC plate and run in the system *n*-butanol/acetic acid/water (3.5:1:2, v/v). Plates were dried, briefly stained with Coomassie Blue, and washed with water.

C-laurdan Spectroscopy—Cell membrane, liposome, and proteoliposome amounts were standardized to scattering fluorescence emission at 425 nm (λ_{ex} 385 nm) (26). This emission intensity relates directly to membrane amount as judged by phosphate assay (supplemental Fig. S5). Following standardization to 30,000 intensity units, membranes were stained with 100 μM C-laurdan and incubated for 15 min at room temperature to equilibrate (11). C-laurdan was then excited at 385 nm. All spectra were recorded twice, averaged, and background-subtracted. This was repeated three times per sample. The general polarization (GP) value was calculated from the following emission bands: (Ch1) 400–460 nm and (Ch2) 470–530 nm according to Parasassi *et al.* (27):

$$GP = \frac{I_{Ch1} - I_{Ch2}}{I_{Ch1} + I_{Ch2}} \quad \text{(Eq. 1)}$$

All spectra were recorded with 1 nm resolution on a fluorescence spectrometer (Fluoromax-3, Horriba, Kyoto, Japan) with a Thermo-Haake thermostat (Karlsruhe, Germany) at 23 °C.

Membrane Solubilization Analysis—Because scattering fluorescence emission intensity at 425 nm (λ_{ex} 385 nm) reports membrane amount (supplemental Fig. S5), it also decreases as a function of membrane solubilization by detergent. Resistance to detergent solubilization is known to correlate membrane order and robustness (28) and was in this way measured for bacterial and eukaryotic surface membranes (with or without

[2] The abbreviations used are: POPC, 1-palmitoyl-2-oleoyl-*sn*-glycero-3-phosphocholine; POPG, 1-palmitoyl-2-oleoyl-*sn*-glycero-3-phospho-(1′-*rac*-glycerol); POPE, 1-palmitoyl-2-oleoyl-*sn*-glycero-3-phosphoethanolamine; SM, sphingomyelin; DDM, dodecyl maltoside; laurdan, 6-dodecanoyl-2-dimethylaminonapthalene; C-laurdan, 6-dodecanoyl-2-methylcarboxymethylaminonapthalene; GP, generalized polarization; Lo, model membrane liquid-ordered phase; Ld, model membrane liquid disordered phase; TM, transmembrane.

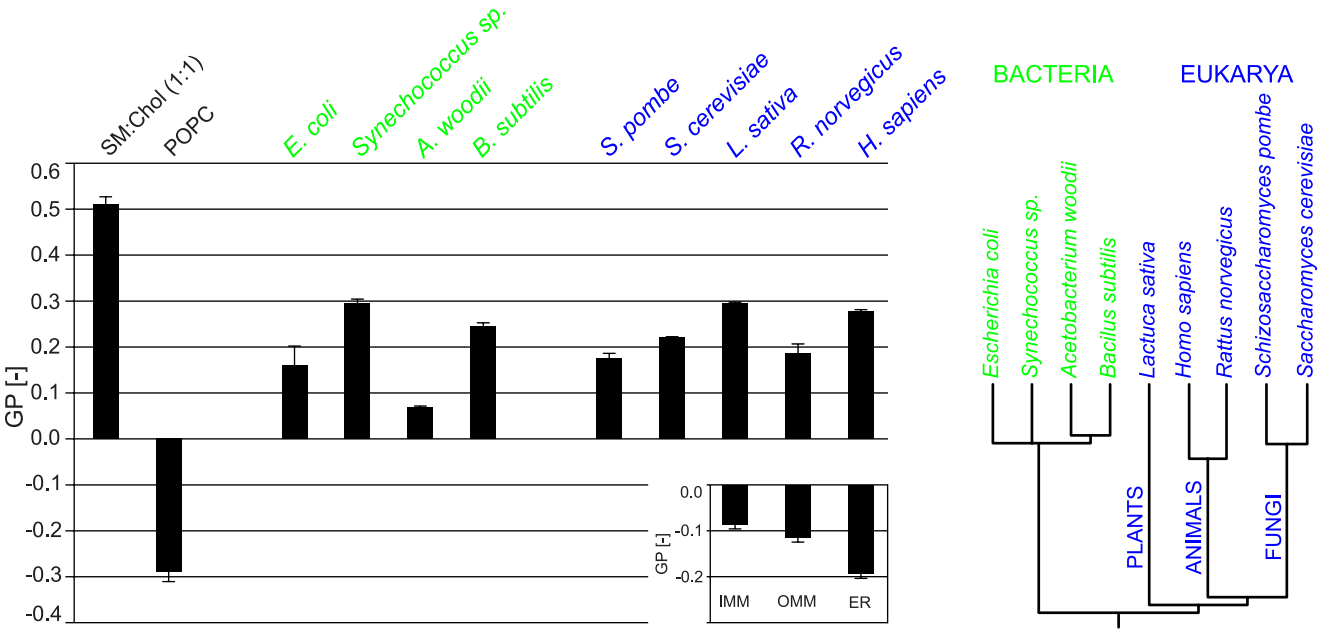

FIGURE 1. **Evolutionary convergence of cell surface order.** The limiting membranes of bacteria and sterol-containing eukaryotes were prepared and evaluated by C-laurdan spectroscopy. This index of lipid packing is presented as a GP value (mean ± S.D., $n = 3$), ranging from +1 as most ordered and −1 as least ordered. Samples are scaled against liposome standards for Lo phase (*SM/Chol, 1:1*), Ld phase (*POPC*), and internal eukaryotic membranes (*inset*: inner mitochondrial membrane (*IMM*); outer mitochondrial membrane (*OMM*); and endoplasmic reticulum (*ER*)). The order of the cell surface converges to a positive GP range, independent of taxonomic distinction and evolution of membrane-rigidifying cholesterol.

protein) along with their counterpart-reconstituted systems. *E. coli* inner membrane and RBC plasma membrane preparations were extruded to 100 nm vesicles and then adjusted in concentration to match the scattering fluorescence given by the 100 nm liposomes made from their extracted lipids (for bacterial membrane, starting emission intensity = 25,000 units; for erythrocyte membrane, starting emission intensity = 40,000 units). For their reconstituted counterpart systems (bacterial = POPG ± TM peptide; eukaryotic = POPC/cholesterol/SM ± TM peptide) membranes were standardized to 80,000 intensity units. Increasing concentrations of DDM were then added. For RBC membranes (with or without protein), starting DDM concentration = 0.008% (w/v) and was sequentially increased by 0.008%; for *E. coli* membranes (with or without protein), starting DDM concentration = 0.004% (w/v) and was sequentially increased by 0.004%; for model membranes (liposomes *versus* proteoliposomes), starting DDM concentration = 0.016% (w/v) and was sequentially increased by 0.016%. Detergent titrations were repeated three times for each sample.

RESULTS AND DISCUSSION

Order of Eukaryotic and Bacterial Plasma Membranes—The fluorescence spectroscopy of membranes stained with the lipid dye laurdan, and in particular with its more water-soluble analog C-laurdan (29), has emerged as a robust method to measure order, both for model membrane systems and cell membrane preparations (11, 30, 31). Reported as a GP value, this index of lipid packing is of arbitrary units and theoretically ranges from +1 as most ordered and −1 as least ordered (27).

We used this technique to measure lipid packing in plasma membranes prepared from a number of eukaryotic and bacterial sources. Live cell staining was not employed due to photoselectivity effects (11). Membrane content was measured by the scattering of fluorescence light at 425 nm (λ_{ex} 385 nm) (Ref. 26 and supplemental Fig. S5) and standardized to the amount of C-laurdan added (11). The resultant GP values were scaled against the known extrema of order in wholly liquid membranes (11): pure liquid-ordered/Lo phase (SM/cholesterol, 1:1, v/v; GP = 0.5 ± 0.017) and pure liquid disordered/Ld phase (POPC; GP = −0.29 ± 0.020) (supplemental Fig. S6). We find that, irrespective of whether the surface membranes contained sterol, all converged on similar values with a positive GP value (Fig. 1). This level of ordering was notably greater than the pure POPC bilayer and eukaryotic internal membranes, consistent with densely packed plasma membranes that confer robustness at all cell boundaries. At the other extreme, membrane order was well below that of the SM/cholesterol bilayer. This indicates that, although high order seems to be an important surface feature, it is kept below the maximum order achievable for fluid lipid-only membranes, perhaps indicative of the fact that it must not exceed levels that may compromise functional membrane fluidity. This is consistent with the fact that Lo membrane reduces inclusion of most transmembrane proteins (32). Taken together, it appears that eukaryotic and bacterial surface membrane orders have converged on a similar level. As the conservation of fluidity is considered a universal attribute of cell membrane functionality (5, 6, 33–36) evolutionary convergence of membrane order is functionally predictable. Structurally, however, membrane-rigidifying cholesterol is unique to eukaryotes, and work from model systems predicts that bilayers with or without sterol are incapable of producing similar membrane order (3, 37).

Molecular Origins of Membrane Order—To address this issue, we investigated in more detail the structure of two bacterial and eukaryotic surface membrane preparations for which

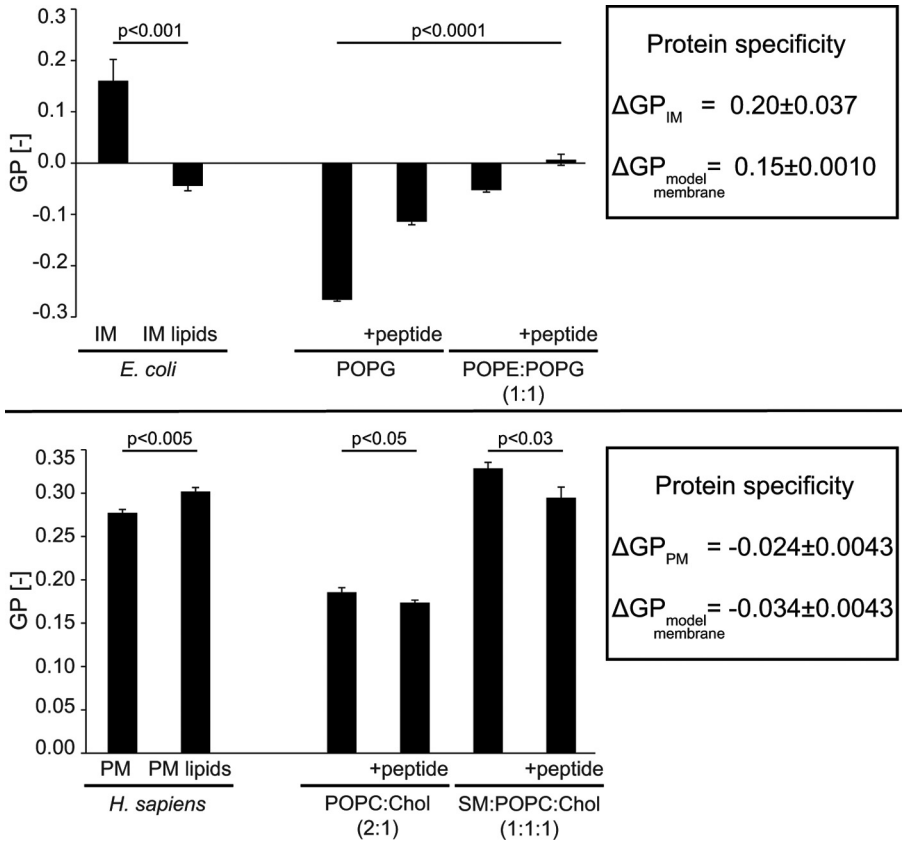

FIGURE 2. **Organization of order in *E. coli* inner membrane (*IM*) (*upper panel*) and human RBC plasma membrane (*lower panel*).** For both cases, order of the intact surface membrane was compared with membranes formed from their extracted lipids (two sided *t*-tests). The corresponding bidirectional effect of a model peptide was then reconstituted into membranes formed from lipids of inner membrane (PG/PE) (ANOVA: $p < 0.0001$; with Tukey's test: POPG *versus* POPG/peptide, $p < 0.01$; POPG *versus* POPG/POPE, $p < 0.01$; POPG *versus* POPG/POPE/peptide, $p < 0.01$; POPG/peptide *versus* POPG/POPE, $p < 0.05$; POPG/peptide *versus* POPG/POPG/peptide, $p < 0.05$; POPG/POPE *versus* POPG/POPE/peptide, $p < 0.05$) and plasma membrane (SM/PC/cholesterol) (two sided *t*-tests). This contribution of protein to membrane order is summarized as ΔGP_{PM} or ΔGP_{IM} = GP intact cell membrane minus GP cell membrane lipids only and $\Delta GP_{model\ membrane}$ = GP proteoliposome (TM peptide + POPG or SM/POPC/Chol) minus GP liposome (POPG or SM/POPC/Chol). GP values represent mean ± S.D. ($n = 3$).

there is the most structural and compositional information: the inner membrane of *E. coli* and human RBC ghosts. We began by comparing membrane order in the intact preparation to membranes made from their extracted lipids only. In the bacterial condition, lipid composition alone failed to confer positive GP (Fig. 2), suggesting that proteins contribute significantly to structural robustness. Indeed, inflexible TM protein segments are known to increase membrane order by limiting conformational movement of lipids (38, 39). Moreover, it has been suggested that the large oligomeric protein complexes of the bacterial inner membrane provide an additional source of membrane structure and rigidity (13). However, in the eukaryotic condition, the order of the lipid membranes without protein exceeded that of the intact plasma membrane preparation (Fig. 2), indicating that in this case the protein reduced the membrane order potentiated by the eukaryotic lipids. RBC membranes are likely comparable to bacteria in terms of their high protein density (13, 40), suggesting that the rigidifying property of membrane proteins is context-specific. This destabilizing effect, although small in the RBC membranes, was confirmed to a much larger extent in ergosterol-containing yeast plasma membranes (supplemental Fig. S8) suggesting that it may be a general feature of sterol membranes. Interestingly, experiments employing electron spin resonance and measures of phase transition temperatures have also revealed disruption of eukaryotic lipid ordering by plasma membrane protein (41, 42).

Reconstitution of Ordered Membranes—To investigate the molecular basis for this bifunctionality in membrane ordering, we used a synthetic hydrophobic peptide as a generic TM protein substitute that forms a TM helix when reconstituted into bilayers (43, 44). It was reconstituted to physiological concentrations (3 mol% (Refs. 39 and 40)) into liposomes made from the lipids of either bacterial inner membrane (IM) (phosphatidylglycerol (PG) and phosphatidylethanolamine (PE) (21)) or eukaryotic plasma membrane (POPC/SM/cholesterol) (22). In both cases verification of peptide integration was obtained by a proteinase K protection assay (supplemental Fig. S7). We found that in the sterol-free case, the peptide increased membrane order (Fig. 2), consistent with model membrane studies (16, 45, 46). Here, the peptide integration accounts for almost the same order difference we observe for the inner membrane preparation with removed protein ($\Delta GP_{IM} = 0.20 \pm 0.04$ *versus* $\Delta GP_{model\ membrane} = 0.15 \pm 0.01$). This indicates that the addition of a generic TM protein segment to a simple PG bilayer can contribute an increase in lipid packing as seen in the isolated bacterial membrane. Interestingly, the combination of PG and PE also increases membrane order compared with PG alone

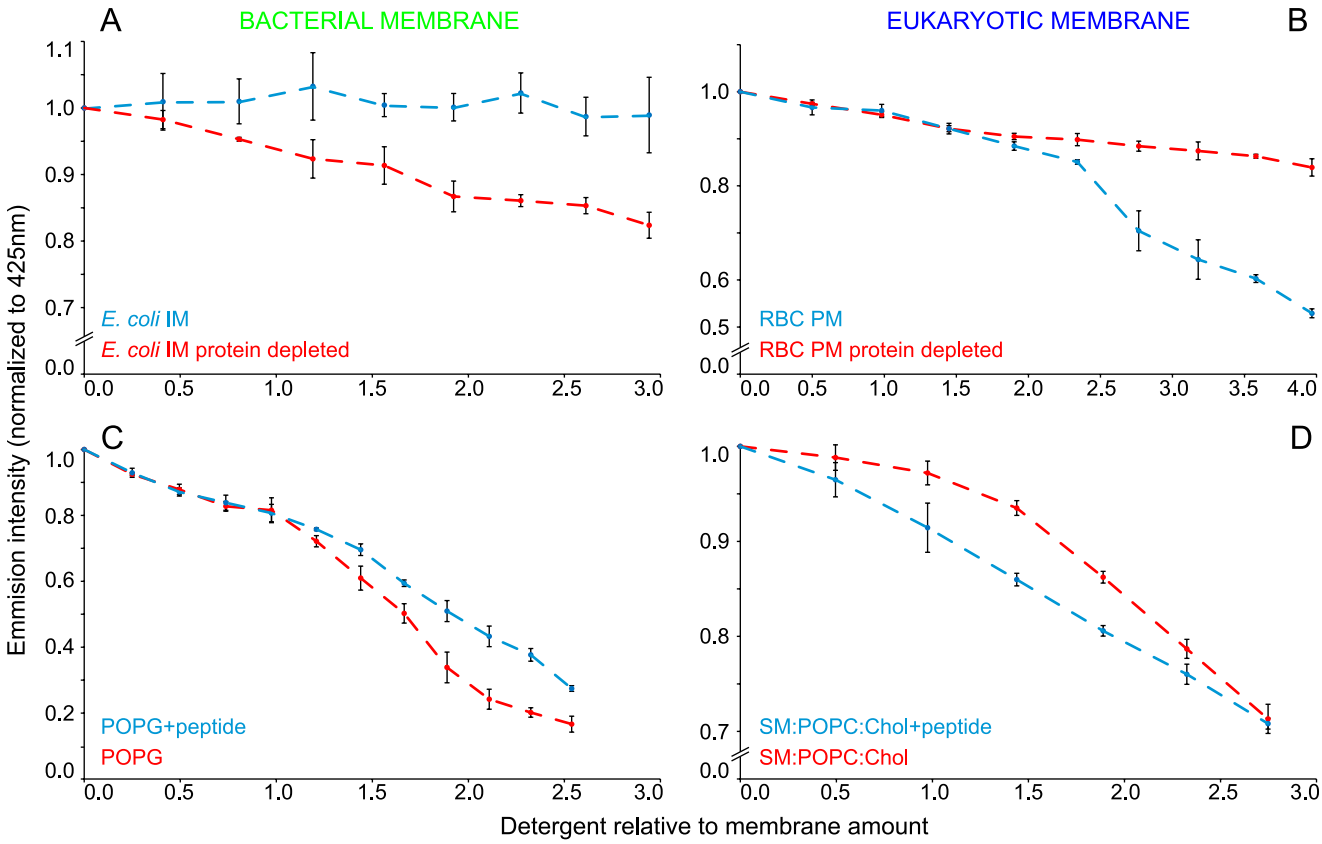

FIGURE 3. **Membrane protein bifunctionality revealed by differential resistance to detergent.** To determine the nature by which membrane protein influences mechanical robustness at the cell surface, susceptibility to solubilization by DDM was measured for membranes extruded to 100 nm: *E. coli* inner membrane with or without protein (*A*) and RBC plasma membrane with or without protein (*B*). These cases were also reconstituted by incorporating a synthetic TM peptide into 100 nm membranes formed from the sterol-free lipids of bacterial inner membrane (*C*) or sterol-containing eukaryotic plasma membrane (*D*). Data are presented as unsolubilized membrane amount (*ordinate*; scatter intensity normalized to emission at 425 nm (λ_{ex} 385 nm)) *versus* relative detergent concentration (*abscissa*; (%DDM/initial membrane scatter intensity) * 100). The values are mean ± S.D., $n = 3$.

(Fig. 2). This is suggestive of a headgroup-limited spacing, where the small ethanolamine slips underneath the large glycerol headgroup, perhaps akin to the eukaryotic "umbrella effect" in which cholesterol tightly packs under membrane lipids with large headgroups (47). As such, lipid and protein specificities appear additive, suggesting that the conserved regime of surface ordering seen in sterol-lacking bacteria may be achieved via the cooperation between lipid and protein-derived ordering. In contrast, incorporation of the same peptide to cholesterol-containing lipid systems resulted in a decrease in sterol-derived membrane order (Fig. 2). Membrane ordering both by sterol and by sterol-sphingolipid combination has been well documented (7–9, 11); however, the disordering effect of peptide incorporation into such systems is beginning to emerge as a new theme. This work suggests that disorder may arise from disruption of lipid packing either by hydrophobic mismatch between protein transmembrane segments and the bilayer or by protruding side chains on the helix surface (16, 17, 48, 49). Reconstitution of the model peptide into cholesterol-containing model membranes also generated a similar protein specificity to that observed for the native red blood cell system, albeit now eliciting a reduction in GP ($\Delta GP_{PM} = -0.024 \pm 0.0042$ *versus* $\Delta GP_{model\ membrane} = -0.034 \pm 0.0043$).

Our data indicate that, unlike bacteria, the source of eukaryotic membrane ordering is mainly via lipid interactions involving sterol and sphingolipid; this view is consistent with both model and cell membrane studies (9, 50, 51). In this context, lipid-derived order is prevented from exceeding the functionally relevant surface order membrane regime by transmembrane protein-dependent disordering. This suggests that membrane proteins can "buffer" bacterial and eukaryotic lipid composition to the surface membrane order regime.

Membrane Robustness—Having identified lipid context as the basis for ordering and disordering by protein, we tested whether this bifunctionally could be confirmed by resistance to membrane detergent. Detergent resistance is a measure that relates directly to lipid packing (28) and would be predicted to correlate with the C-laurdan ordering results of the *E. coli* inner membrane and RBC plasma membrane. To this end we measured DDM-mediated solubilization of uniform, 100 nm vesicles (extruded from native membranes and membranes reconstituted from their extracted lipids) as a decrease in the scattering of fluorescence light at 425 nm (λ_{ex} 385 nm) (26). The scattering signal correlated well with vesicle concentration and was used to adjust membrane amounts to the same level (supplemental Fig. S5). In the applied detergent concentration ranges, we observed resistance to solubilization for native *E. coli* membranes but not for protein-free *E. coli* membranes (Fig. 3). In contrast, the native RBC membranes exhibited a faster onset of solubilization than did their protein-free coun-

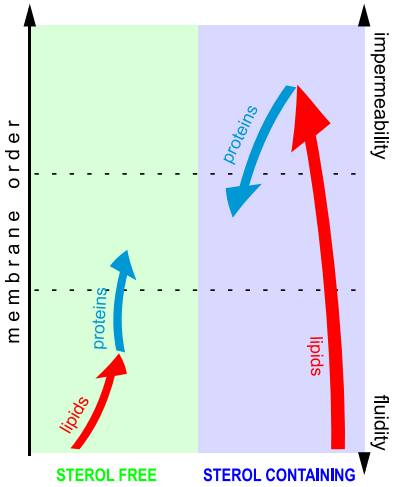

FIGURE 4. **Transmembrane protein as a buffer for membrane order and robustness at the cell surface.** The functional range of order seen at the cell surface may represent a balance between enhancing packing in the hydrocarbon core to resist rupture and leakage and maintaining the level of fluidity needed to support membrane bioactivity. Convergence to this order regime could be achieved in two ways. In the absence of sterol, lipids and proteins act cooperatively to drive hydrocarbon chain packing, with transmembrane protein providing a rigid surface upon which acyl chains are ordered. In sterol-containing membranes, the same protein input now disrupts sterol-acyl chain alignment, placing an upper limit on ordering by eukaryotic lipids.

terparts (Fig. 3). This suggested that the packing state of the membrane indeed reflects structural robustness and that the dual nature by which membrane proteins organize order also regulates resistance to solubilization. Moreover, we were able to reconstitute the same protein bifunctionality in our minimal model membrane systems: sterol-free liposomes were more efficiently solubilized in the absence of model TM peptide, whereas sterol-containing POPC/SM/cholesterol liposomes were more efficiently solubilized if the same TM peptide was incorporated (Fig. 3). This bi-directionality in protein effects supports our previous assertion that proteins can act oppositely to tune order, and therefore structural robustness.

Conclusions and Perspectives—In the eukaryotic and bacterial domains of life there exists a similar degree of lipid packing at the cell surface. Evolutionary convergence to this surface order regime likely reflects the preservation of a functional condition: a densely packed hydrocarbon core endowing the membrane with reduced permeability and higher resistance to mechanical forces, all at a level of order that is still compatible with the lateral mobility needed to support membrane bioactivity. Our data suggest that this convergence could involve the action of transmembrane proteins, albeit in two distinct roles (Fig. 4). In the absence of sterol, transmembrane proteins drive lipid packing, very likely acting in a similar way to cholesterol: providing a rigid surface in a sea of highly flexible acyl chains. In sterol-containing membranes, there now appears to be an antagonistic relationship in which transmembrane proteins place an upper limit on eukaryotic lipid order, most likely via the breaking of sterol-acyl chain alignment. Bidirectional ordering by membrane protein is a physical principle that, although it does not account for variations in lipid subclass or protein oligomerization behaviors, it emphasizes cell membranes as a protein-lipid composites, which despite radically distinct compositions (*e.g.* inter-species/cell type variation) can be tuned to yield similar barrier properties.

Acknowledgments—We thank Ünal Coskun and Barbara Borgonovo (Max Planck Institute for Molecular Biology and Genetics, Dresden, Germany) for technical assistance, Erhard Bremer (Philipps-Universität Marburg, Germany) for providing the B. subtilis strain, Kristina Hölig (Technische Universität, Dresden, Germany) for collection of blood samples, and Jarosław Króliczewski (University of Wrocław, Poland) for providing Synechococcus sp. strain.

REFERENCES

1. Tanford, C. (1978) *Science* **200,** 1012–1018
2. Noireaux, V., Maeda, Y. T., and Libchaber, A. (2011) *Proc. Natl. Acad. Sci. U.S.A.* **108,** 3473–3480
3. Bloch, K. E. (1983) *CRC Crit. Rev. Biochem.* **14,** 47–92
4. Mouritsen, O. G., and Bloom, M. (1993) *Annu. Rev. Biophys. Biomol. Struct.* **22,** 145–171
5. Hazel, J. R. (1995) *Annu. Rev. Physiol.* **57,** 19–42
6. Sajbidor, J. (1997) *Crit. Rev. Biotechnol.* **17,** 87–103
7. Veatch, S. L., and Keller, S. L. (2005) *Phys. Rev. Lett.* **94,** 148101
8. Feigenson, G. W. (2009) *Biochim. Biophys. Acta* **1788,** 47–52
9. Niemelä, P. S., Hyvönen, M. T., and Vattulainen, I. (2009) *Biochim. Biophys. Acta* **1788,** 122–135
10. Mitra, K., Ubarretxena-Belandia, I., Taguchi, T., Warren, G., and Engelman, D. M. (2004) *Proc. Natl. Acad. Sci. U.S.A.* **101,** 4083–4088
11. Kaiser, H. J., Lingwood, D., Levental, I., Sampaio, J. L., Kalvodova, L., Rajendran, L., and Simons, K. (2009) *Proc. Natl. Acad. Sci. U.S.A.* **106,** 16645–16650
12. Smith, W. L., Garavito, R. M., and Ferguson-Miller, S. (2001) *J. Biol. Chem.* **276,** 32393–32394
13. Engelman, D. M. (2005) *Nature* **438,** 578–580
14. Jacobson, K., Mouritsen, O. G., and Anderson, R. G. (2007) *Nat. Cell Biol.* **9,** 7–14
15. Lingwood, D., Ries, J., Schwille, P., and Simons, K. (2008) *Proc. Natl. Acad. Sci. U.S.A.* **105,** 10005–10010
16. Nezil, F. A., and Bloom, M. (1992) *Biophys. J.* **61,** 1176–1183
17. Simons, K., and Vaz, W. L. (2004) *Annu. Rev. Biophys. Biomol. Struct.* **33,** 269–295
18. Lewis, B. A., and Engelman, D. M. (1983) *J. Mol. Biol.* **166,** 203–210
19. Huschilt, J. C., Millman, B. M., and Davis, J. H. (1989) *Biochim. Biophys. Acta* **979,** 139–141
20. de Planque, M. R., Greathouse, D. V., Koeppe, R. E., 2nd, Schäfer, H., Marsh, D., and Killian, J. A. (1998) *Biochemistry* **37,** 9333–9345
21. Ruiz, N., Kahne, D., and Silhavy, T. J. (2006) *Nat. Rev. Microbiol.* **4,** 57–66
22. Kalvodova, L., Sampaio, J. L., Cordo, S., Ejsing, C. S., Shevchenko, A., and Simons, K. (2009) *J. Virol.* **83,** 7996–8003
23. Ejsing, C. S., Sampaio, J. L., Surendranath, V., Duchoslav, E., Ekroos, K., Klemm, R. W., Simons, K., and Shevchenko, A. (2009) *Proc. Natl. Acad. Sci. U.S.A.* **106,** 2136–2141
24. Sampaio, J. L., Gerl, M. J., Klose, C., Ejsing, C. S., Beug, H., Simons, K., and Shevchenko, A. (2011) *Proc. Natl. Acad. Sci. U.S.A.* **108,** 1903–1907
25. Kalvodova, L., Kahya, N., Schwille, P., Ehehalt, R., Verkade, P., Drechsel, D., and Simons, K. (2005) *J. Biol. Chem.* **280,** 36815–36823
26. Castanho, M. A. R. B., Santos, N. C., and Loura, L. M. S. (1997) *Eur. Biophys. J.* **26,** 253–259
27. Parasassi, T., De Stasio, G., d'Ubaldo, A., and Gratton, E. (1990) *Biophys. J.* **57,** 1179–1186
28. Schroeder, R. J., Ahmed, S. N., Zhu, Y., London, E., and Brown, D. A. (1998) *J. Biol. Chem.* **273,** 1150–1157
29. Kim, H. M., Choo, H. J., Jung, S. Y., Ko, Y. G., Park, W. H., Jeon, S. J., Kim, C. H., Joo, T., and Cho, B. R. (2007) *Chembiochem* **8,** 553–559
30. Dietrich, C., Bagatolli, L. A., Volovyk, Z. N., Thompson, N. L., Levi, M., Jacobson, K., and Gratton, E. (2001) *Biophys. J.* **80,** 1417–1428
31. Klemm, R. W., Ejsing, C. S., Surma, M. A., Kaiser, H. J., Gerl, M. J., Sam-

paio, J. L., de Robillard, Q., Ferguson, C., Proszynski, T. J., Shevchenko, A., and Simons, K. (2009) *J. Cell Biol.* **185,** 601–612
32. Lingwood, D., and Simons, K. (2010) *Science* **327,** 46–50
33. Sinensky, M. (1974) *Proc. Natl. Acad. Sci. U.S.A.* **71,** 522–525
34. Macdonald, A. G., and Cossins, A. R. (1985) *Symp. Soc. Exp. Biol.* **39,** 301–322
35. Chintalapati, S., Kiran, M. D., and Shivaji, S. (2004) *Cell Mol. Biol.* **50,** 631–642
36. Mykytczuk, N. C., Trevors, J. T., Leduc, L. G., and Ferroni, G. D. (2007) *Prog. Biophys. Mol. Biol.* **95,** 60–82
37. Mouritsen, O. G., and Zuckermann, M. J. (2004) *Lipids* **39,** 1101–1113
38. Jähnig, F. (1981) *Biophys. J.* **36,** 329–345
39. Seelig, J., and Seelig, A. (1980) *Q. Rev. Biophys.* **13,** 19–61
40. Dupuy, A. D., and Engelman, D. M. (2008) *Proc. Natl. Acad. Sci. U.S.A.* **105,** 2848–2852
41. Ge, M., Gidwani, A., Brown, H. A., Holowka, D., Baird, B., and Freed, J. H. (2003) *Biophys. J.* **85,** 1278–1288
42. Levental, I., Lingwood, D., Grzybek, M., Coskun, U., and Simons, K. (2010) *Proc. Natl. Acad. Sci. U.S.A.* **107,** 22050–22054
43. Ren, J., Lew, S., Wang, J., and London, E. (1999) *Biochemistry* **38,** 5905–5912
44. Fastenberg, M. E., Shogomori, H., Xu, X., Brown, D. A., and London, E. (2003) *Biochemistry* **42,** 12376–12390
45. Killian, J. A., and Nyholm, T. K. (2006) *Curr. Opin. Struct. Biol.* **16,** 473–479
46. Holt, A., and Killian, J. A. (2010) *Eur. Biophys. J.* **39,** 609–621
47. Huang, J., Buboltz, J. T., and Feigenson, G. W. (1999) *Biochim. Biophys. Acta* **1417,** 89–100
48. Lundbaek, J. A., Andersen, O. S., Werge, T., and Nielsen, C. (2003) *Biophys. J.* **84,** 2080–2089
49. Kaiser, H. K., Orłowski, A., Róg, T., Nyholm, T., Chai, W., Feizi, T., Lingwood, D., Vattulainen, I., and Simons, K. (2011) *Proc. Natl. Acad. Sci. U.S.A.* **108,** 16628–16633
50. Lönnfors, M., Doux, J. P., Killian, J. A., Nyholm, T. K., and Slotte, J. P. (2011) *Biophys. J.* **100,** 2633–2641
51. Surma, M. A., Klose, C., Klemm, R. W., Ejsing, C. S., and Simons, K. (2011) *Traffic* **12,** 1139–1147

Supplementary Information: methods, references, figure captions and figures

Molecular convergence of bacterial and eukaryotic surface order

Hermann-Josef Kaiser[1], Michal A. Surma[1], Florian Mayer[2], Ilya Levental[1], Michal Grzybek[1], Robin W. Klemm[3], Sandrine Da Cruz [4], Chris Meisinger[5,6] ,Volker Müller[2], Kai Simons[1] and Daniel Lingwood[1].

[1]Max Planck Institute for Molecular Cell Biology and Genetics, Pfotenhauerstr. 108, 01307 Dresden, Germany
[2]Department of Molecular Microbiology & Bioenergetics, Institute of Molecular Biosciences, Goethe-Universität Frankfurt, Max-von-Laue-Str. 9, 60438 Frankfurt am Main, Germany
[3]Harvard Medical School, 240 Longwood Ave., Boston, MA 02115, USA
[4]Ludwig Institute for Cancer Research, University of California San Diego, 9500 Gilman Drive, Cellular and Molecular Medicine - East, 3041, San Diego La Jolla, California, USA
[5]Institut für Biochemie und Molekularbiologie, ZBMZ, Universität Freiburg, D-79104 Freiburg, Germany
[6]BIOSS Centre for Biological Signaling Studies, Universität Freiburg, 79104 Freiburg, Germany

Present address, Daniel Lingwood:

Vaccine Research Center, National Institute of Allergy and Infectious Diseases, National Institutes of Health, Bethesda, MD 20892-3005, USA.

Surface membrane preparation protocols

E. coli inner membrane preparation

Inner membranes were prepared as described (1). *E.coli* (DH5α) were grown to an OD_{600} of 0.3 and resuspended in 60 mL of suspension buffer [250mM sucrose + 50mM HEPES + 1mM EDTA + 1mM DTT + protease inhibitor cocktail (1 pellet /60ml; Roesch) +benzonase (400U)]. Suspension was cooled to 4°C and passed three times through high-pressure cell homogenizer (Emulsiflex, 15000psi). Cell debris was then pelleted (10000g, 30min). The samples were then centrifuged at 16000g for 20 min and then 165000g for 2h. The membrane pellet was resuspended (dounce homogenizer, 10 strokes) and centrifuged through a five step sucrose gradient (0.6 M to 1.4 M, in suspension buffer) at 165000g for 18h. Inner membrane, which does not sediment under these conditions (1), was collected frozen at -80°C for subsequent analysis. Inner membrane enrichment was confirmed by lack of phospholipase A2 activity (outer membrane marker), as judged by the processing of exogenously added rhodamine-DOPE (Fig. S1).

Bacillus subtilis surface membrane

Membranes were prepared according to a modification of Konings et al. (2). *B. subtilis* (168 trp+) were grown to an OD_{600} of 0.3 and resuspended in 60 mL of suspension buffer [250mM sucrose + 50mM HEPES + 1mM EDTA + 1mM DTT + protease inhibitor cocktail (1 pellet /60ml; Roesch) +benzonase (400U)] + lysozyme (500μg/ml). The cells were incubated for 30 min at room temperature, was cooled to 4°C and passed three times through high-pressure cell homogenizer (Emulsiflex, 15000psi). Cell debris was then pelleted (10000g, 30min). The samples were then centrifuged at 16000g for 30 min

and then 165000g for 2h, washed (160000g, 2h), and finally resuspended in storage buffer and frozen at -80°C for subsequent analysis.

A. woodi surface membrane

Membrane preparation was according to Imkamp et al. (3). Briefly, cells were grown to an OD_{600} of 0.3, resupended in 150ml lysozyme buffer (50 mM imidazole-HCl, 20mM $MgSO_4$, 5mM dithioerythritol, 0.14g/ml of saccharose; pH 8.0) with 0.8 g lysozyme and then shaken for 1.5h at 37°C. The sample was then centrifuged (9800g, 20 min), resuspended in 20 ml storage buffer (50mM imidazole-HCl, 20mM MgSO, 0.14g/ml of saccharose; pH 7.0) and then disrupted by French Press (3 passages, 1000psi). The suspension was adjusted to 150 ml, and centrifuged to pellet cell debris (15000g, 20 min). The supernatent was then centrifuged to pellet cell membranes (160000g, 2h), the pellet was then washed (160000g, 2h) and then resuspended in storage buffer. Samples were and frozen at -80°C for subsequent analysis.

Cyanobacteria Synechococcus sp. surface membrane

Cyanobacteria *Synechococcus* sp. PCC 7002 surface membrane was purified according to Murata & Omata (4). Cyanobacteria were cultivated in the medium A (5) supplemented with A5+Co trace metal mix (6) at 39°C in the atmosphere containing 5% CO_2 and with stirring under appr. 500 lux white light illumination to mid. log. phase and harvested afterwards by 10 min centrifugation (5000g), washed once with water and frozen as pellets at -80°C until further processing. Three grams of frozen pellet were thawed and resuspended in 30 ml HEPES-KOH buffer, pH 7 with 600mM sucrose, 2mM EDTA and

0.03% lysozyme and incubated at 30°C under room light and with gentle agitation for 2 h. Afterwards cells were collected in 5000g, 5 min spin and washed twice with 20mM HEPES-KOH, pH=7 with 600mM sucrose and finally resuspended in 30 ml volume. Suspension was cooled to 4°C and passed three times through high-pressure cell homogenizer (Emulsiflex, 15000psi). Immediately 500ul of 10mM sodium acetate, pH 5.6 with 1mM $MgCl_2$ and benzonase (250u/µl, Novagen), CLAP [chymostatin, leupeptin, antipain, and pepstatin] and 1 mM PMSF was added to the homogenate and everything was incubated on ice for 15 min. Afterwards remaining were pelleted for 10 min at 5000g (4°C) and supernatant was adjusted to 50% sucrose (w/v) using 90% (w/v) sucrose solution in 24mM HEPES-KOH, pH 7; 12mM EDTA, 24mM NaCl and 17 ml were bottom-loaded on step sucrose gradient (8ml of 39% [w/v] 3ml of 30% [w/v] and 7ml of 10% [w/v] sucrose in 10mM HEPES-KOH, pH 7; 5mM EDTA, 10mM NaCl). The gradient was spun with RCF_{max} 130000g at 4°C in a swing-out rotor (SW28 Beckman Coulter) for 16h. Gathered in the visible band in the 30% sucrose yellow PM was carefully collected, diluted with 150 mM NH_4HCO_3 and spun down for 1 h with RCF_{max} 193000g (SW40 Beckman Coulter; 4°C). Pellet was resuspended again in 150mM NH_4HCO_3 and spun 1h with RCF_{max} 186000g at 4°C in TLA55, Beckman Coulter rotor. The pellet was then resuspended in 50 mM HEPES/150 mM NaCl, pH 7.4 and frozen at -80°C for subsequent analysis. With this procedure we report a B-caretonoid/chlorophyll ratio of 4, consistent with surface membrane enrichment (7).

Saccharomyces cerevisiae plasma membrane

Plasma membrane (PM) was prepared as described (8, 9). Yeast (BY4741 strain) were cultivated overnight at 30°C in YEPD to mid. log. phase, harvested by 4000g, 4 min centrifugation and resuspended in 4 ml of lysis buffer (800 mM sorbitol, 1mM EDTA, 10mM triethanolamine, pH 7.4, CLAP [chymostatin, leupeptin, antipain, and pepstatin], 1mM PMSF). Then yeast were disrupted at 4°C with 0.5 mm zirconia beads (BioSpec Products, Inc.) and spun down for 10min at 2000g (4°C). The supernatant was centrifuged for another 30 min at 20000g (4°C), which produced the pellet P20. The pellet was resuspended 300µl of 20% glycerol, pH 5, and loaded on top of a 4ml step gradient (1.3 ml of 55% [w/w] sucrose and 2.7ml of 45% [w/w] sucrose in 10mM triethanolamine, pH 7.4). The gradient was spun with RCF_{max} 129000g at 4°C in a swing-out rotor (SW60; Beckman Coulter) for 5h. Gathered in the visible band at the 45%/55% gradient interface membranes were carefully collected, diluted with 20% glycerol, pH 5 and pelleted (1h spin with RCF_{max} 186000g at 4°C in TLA55, Beckman Coulter rotor). The pellet was resuspended in 300µl of 20% glycerol and loaded on a second step gradient (55%/45% sucrose) and centrifuged for 16 h in the same conditions as previously. Visible 45%/55% interface band was collected, diluted with 150mM NH_4HCO_3 and spun down in TLA55 rotor as previously. The obtained PM pellet was resuspended in the same solution and spun down again to wash it. The pellet was then resuspended in 50mM HEPES/150 mM NaCl, pH 7.4 and frozen at -80°C for subsequent analysis. Western blots for membrane markers were consistent with plasma membrane enrichment (Fig S2).

Saccharomyces pombe plasma membrane

S. pombe WT L972 h- strain PM was purified as described (10). Yeast were cultivated overnight at 30°C in YES to mid. log. phase, harvested in 4000g, 4min spin and resuspended in 4 ml of lysis buffer (0.25 M sucrose, 50 mM Tris-HCl, pH 7.5, CLAP [chymostatin, leupeptin, antipain, and pepstatin], 1 mM PMSF). Then yeast were disrupted at 4°C with 0.5 mm zirconia beads (BioSpec Products, Inc.) and spun down 2 times for 5 min at 1000g (4°C), followed by 5 min at 3000g (4°C) each time pellets being discarded. The acquired supernatant was spun again for 40 min at 15000g (4°C) and the obtained pellet was resuspended in 10 mM Tris-CH_3COOH, 1mM EDTA, pH 5.2 to final protein concentration of 2.5mg/ml and spun for 45 sec in eppendorf swing out rotor at 7500g (4°C). The supernatant was adjusted to pH 7.5 with 1 M NaOH and centrifuged for 12 min with RCF_{max} 45000g [SW60 rotor; Beckman Coulter] (4°C). Obtained pellet was resuspended in 1ml 24% (w/w) sucrose in 10mM Tris-CH_3COOH, pH 7.5 and applied on a top of a 10ml step gradient (5 ml 55% [w/w] sucrose, 3 ml 45% [w/w] sucrose and 2 ml 41% [w/w] sucrose in 10mM Tris-CH_3COOH, pH 7.5), which was spun for 5h with RCF_{max} 100000g [SW40 rotor; Beckman Coulter] (4°C). The visible band at the 45%/55% gradient interface was carefully collected, diluted with 150mM NH_4HCO_3 and pelleted (1h spin with RCF_{max} 186000 g at 4°C in TLA55, Beckman Coulter rotor). The obtained PM pellet was resuspended in the same solution and spun down again to wash it. The pellet was then resuspended in 50mM HEPES/150mM NaCl, pH 7.4 and frozen at -20°C for subsequent analysis.

Plant L. sativa plasma membrane

Plant *L. sativa* PM was prepared by partitioning in two-phase system as described (11). Fresh *L. sativa* was purchased at the local market and 100g of its leaves were homogenized in a blender in 200ml of cold 0.5M sucrose, 50mM HEPES-KOH, pH 7.5, 5mM ascorbic acid, 1mM DTT, 0.6% w/v poly(vinylpyrrolidone) (PVP) buffer with three 20 sec. pulses and obtained pulp was filtered through several layers of cloth. Obtained homoganete was spun down 2 times for 10 min at 10000g (4°C), each time pellet being discarded. The acquired supernatant was spun again for 30 min at 50000g (4°C) and the obtained pellet was resuspended in 10ml 0.33M sucrose, 3mM KCl, 5mM dipotassium phosphate, pH 7.8. Nine grams of this solution was added to 27g of phase mixture to give a final solution of 6.2% w/w dextran T-500, 6.2% w/w PEG 3350, 3mM KCl and 0.33M sucrose (11). The mixture was mix thoroughly by inversing the tube 30 times and phase separation was helped by centrifugation for 5 min at 1500g (4°C). Next 90% of the upper phase was collected and re-applied on fresh lower phase [from the bulk phase system (11)] with 10% of missing upper phase re-added from the fresh bulk phase system. Procedure was repeated two times and the third upper phase was finally diluted 2.5 times with 150mM NH_4HCO_3 and pelleted (1.5h spin with RCF_{max} 186000g at 4°C (SW60; Beckman Coulter) for 1h. The obtained PM pellet was resuspended in smaller volume of the same solution and spun down (1h spin with RCF_{max} 186000g at 4°C in TLA55, Beckman Coulter rotor) again to wash it. The pellet was then resuspended in 50mM HEPES/150mM NaCl, pH 7.4 and frozen at -80°C for subsequent analysis. Following two-phase partitioning, we report a 43% reduction in the chlorophyll to protein ratio, indicating PM enrichment.

Rat basophil leukaemia cell plasma membrane

Plasma membrane vesicles were isolated by N-ethyl maleimide (NEM) vesiculation, described (12, 13). Rat basophil leukaemia (RBL) cells were grown to 70% confluency in a T75 tissue culture flask and exposed to 5ml of vesiculation buffer (10mM HEPES, 150mM NaCl, 2mM $CaCl_2$, 2mM NEM, pH 7.4) for 1h at 37°C. The blebbed vesicles were then concentrated by centrifugation at 20000g for 30 mins after an initial 3 min 150g centrifugation to remove cellular contaminants.

Human red blood cell ghosts

Fresh blood samples were collected from healthy human volunteers (Bereichsleiterin Transfusionsmedizin, Medizinische Klinik und Poliklinik, Technische Univesität, Dresden) and red blood cell (RBC) ghosts were immediately purified at 4°C as described (14). Briefly, cells were washed (10 min, 800g; 10mM Tris-HCl, 120 mM KCl, pH 7.4) to remove the white lymphocyte fraction, resuspended in lysis buffer (5 mM Tris-HCl, 5 mM KCl, 1mM $MgCl_2$, 0.6 mM MgATP, pH 7.4) and then pelleted, (15 min, 15000g). This was repeated until the ghosts were pale pink. Membranes were then pelleted (15 min, 15000g), resuspended in 50 mM HEPES/150 mM NaCl, pH 7.4 and frozen at -80°C for subsequent analysis.

Preparation of eukaryotic internal membranes

Outer mitochondrial membrane

Yeast cells from *S.cerevisiae* were grown at 30°C in YPG medium [1%(w/v) yeast extract, 2% (w/v) Bactopeptone and 3% (w/v) glycerol] until an OD_{600} of approx. 1.5. Cells were harvested and a crude mitochondrial fraction was obtained by differential centrifugation (15). Further purification by a three-step sucrose gradient yielded highly pure mitochondria (15). For generation of mitochondrial membrane fractions 2 mg purified mitochondria were resuspended in 0.5 ml EM buffer (10mM MOPS, 1mM EDTA, pH 7.2) and sonicated 5 x 20 s (80% duty cycle). Membranes were pelleted by centrifugation (100000g, 30 min) and resuspended in 200 µl EM buffer. For isolation of outer membranes 50 mg purified mitochondria were diluted in 25 ml swelling buffer (5mM potassium phosphate, 1mM PMSF, pH 7.4) and incubated on ice for 20 min. Outer membranes were detached by treatment with a glass-Teflon potter (15 strokes) and purified by two consecutive ultracentrifugation steps (sedimentation followed by flotation) on sucrose gradients as described (15). Purified outer membrane vesicles were resuspended in 500 µl EM buffer frozen and at -80°C for subsequent analysis. Western blots for membrane markers were consistent with outer membrane enrichment (Fig. S3).

Inner mitochondrial membrane

Inner mitochondrial membrane from mouse liver preparation was a kind gift from Jean-Claude Martinou (Geneva) and comes directly from the purification developed from their group (16).

Endoplasmic reticulum: dog pancreas rough microsome preparation

Rough microsomes were prepared from freshly excised dog pancreas as described (17). Following tissue homogenization (tissue press and motor driven homogenization in: 250mM sucrose, 50mM TEA, 50mM KOAc, 6mM Mg $(OAc)_2$, 1mM EDTA, 1 mM DTT, 0.5mM PMSF), the sample was centrifuged (10min at 1000g and for 10 min at 10000g) and rough microsomes were pelleted through 10-15 ml 1.3M sucrose cushions in the homogenization buffer (2.5h at 140000g). Pellets were resuspended in 250mM sucrose, 50mM TEA, 1mM DTT using a dounce homogenizer (loose fitting-pestle). To remove absorbed ribosomes and proteins, membranes were passed through a sepharose column in low salt buffer (50mM TEA / 0.5mM Mg (OAc)z / I mM DTT). Turbid fractions were pooled, and the membranes were pelleted by centrifugation (15 min at 50000g) frozen at -80°C for subsequent analysis. Membrane isolation was confirmed by electron microscopy (Fig. S4).

References

SUPPLEMENTARY REFERENCES

1. Rhoads, D.B., Tai, P.C., Davis, B.D. (1984) *J. Bacteriol.* **159,** 63-70
2. Konings, W.N., Bisschop, A., Veenhuis, M., Vermeulen, C.A. (1973) *J. Bacteriol.* **116,** 1456-1465

3. Imkamp, F., Biegel, E., Jayamani, E., Buckel, W., Muller, V. (2007) *J. Bacteriol.* **189,** 8145-8153
4. Murata, N., Omata, T. (1998) *Methods Enzymol.* **167,** 245-251
5. Stevens, S.E.J., Patterson, C.O.P., Myers, J. (1973) *J. Phycol.* **9,** 427-430
6. Rippka, R., Deruelles, J., Waterbury, J.B., Herdman, M., Stainier, R.Y. (1979) *J. Gen. Microbiol.* **111:** 1-61
7. Norling, B., Mirzakhanian, V., Nilsson, F., Morre, D.J., Andersson, B. (1994) *Anal. Biochem.* **218,** 103-111
8. Serrano, R. (1988) *Methods Enzymol.* **157,** 533-544
9. Klemm, R.W., Ejsing, C.S., Surma, M.A., Kaiser, H.J., Gerl, M.J., Sampaio, J.L., de Robillard, Q., Ferguson, C., Proszynski, T.J., Shevchenko, A., Simons, K. (2009) *J. Cell Biol.* **185,** 601-612
10. Dufour, J.P., Goffeau, A. (1978) *J. Biol. Chem.* **253,** 7026-7032
11. Larsson, C., Widell, S., Kjellbom, P. (1987) *Methods Enzymol.* **148,** 558-568
12. Scott, R.E., Perkins, R.G., Zschunke, M.A., Hoerl, B.J., Maercklein, P.B. (1979) *J. Cell Sci.* **35:** 229-243
13. Baumgart, T., Hammond, A.T., Sengupta, P., Hess, S.T., Holowka, D.A., Baird, B.A., Webb, W.W. (2007) *Proc. Natl. Acad. Sci. U.S.A.* **104,** 3165-3170
14. Chorzalska, A., Lach, A., Borowik, T., Wolny, M., Hryniewicz-Jankowska, A., Kolondra, A., Langner, M., Sikorski, A.F. (2010) *Cell Mol. Biol. Lett.* **15,** 406-423
15. Zahedi, R.P., Sickmann, A., Boehm, A.M., Winkler, C., Zufall, N., Schonfisch, B., Guiard, B., Pfanner, N., Meisinger, C. (2006) *Mol. Biol. Cell* **17,** 1436-1450
16. Da Cruz, S., Xenarios, I., Langridge, J., Vilbois, F., Parone, P.A., Martinou, J.C. (2003) *J. Biol. Chem.* **278,** 41566-41571
17. Walter, P., Ibrahimi, I., Blobel, G. (1981) *J. Cell Biol.* **91**, 545-550

SUPPLEMENTARY FIGURE CAPTIONS

Fig. S1. TLC analysis of Rhodamine (Rh)-DOPE processing by *E. coli*. Rh-DOPE (1μg) standard (first lane) is processed into lyso-Rh-DOPE by outer membrane phospholipase A when exposed to *E. coli* cells (middle lane). This activity is not seen when Rh-DOPE was incubated with of inner membrane preparation (IM) (third lane) indicating that IM is depleted for outer membrane. TLC running solvent was 14:6:1 (chloroform/methanol/water, v/v/v).

Fig. S2. Purification of *S. cerevisiae* plasma membrane. Western blot of marker proteins: Gas1p – plasma membrane marker, Dpm1p – ER marker, Sed5p – Golgi apparatus marker, Pep12p – endosomes/trans-Golgi network marker. TCE – total cell extract, G1 – first gradient output, PM – plasma membrane fraction (second gradient output).

Fig. S3. Purification of outer mitochondrial membrane from yeast**.** The final preparation (third lane) was enriched in the outer membrane protein Tom40 and depleted in the matrix protein Mge 1 and inner membrane protein Tim22.

Fig. S4. Transmission electron micrograph of dog pancreatic rough endoplasmic membrane preparation, the classical ER preparation used for *in vitro* translation studies (Walter et al. 1981). Bar = 100nm.

Fig. S5. Fluorescent light scattering membranes (λ_{ex} 385nm) produces a lipid resonance peak (λ_{em} 425nm) that is directly proportional to membrane concentration. This scattering peak correlated directly with the amount of membrane present in solution, as measured by phosphate assay (inset). This scattering signal therefore allowed for precise standardization of membranes purified from different sources (scattering curves of different colours) and also allowed for membrane resistance to detergent to be accurately standardized measured and compared (i.e. between 100nm membranes ± protein).

Fig. S6. Fluorescence spectra of C-laurdan in LUVs show the spectra shift between Lo and Ld membrane (SM:Chol 1:1 and POPC liposomes, respectively). Their respective GP values are the model membrane standards used in this study, representing the extrema of order and disorder in wholly liquid membranes.

Fig. S7. Membrane Incorporation of synthetic peptide. To verify that our LW19/TM peptide was properly incorporated into proteoliposomes, we assayed the degree to which it was protected from digestion by proteinase K. We find that with all lipid compositions proteinase K does not digest the TM peptide, unless the membrane is solubilized by a combination of SDS and Triton X-100, confirming proper membrane integration of the peptide.

Fig. S8. The plasma membrane of S. cerevisiae is disordered by transmembrane protein. C-laurdan spectroscopy was used to measure the order of the intact surface membrane (PM) and compare it to membranes formed from their extracted lipids (PM lipids). Protein-depleted membranes exhibited a substantially greater order value than did the plasma membrane. GP values represent mean ± SD (N=3)

Fig S1

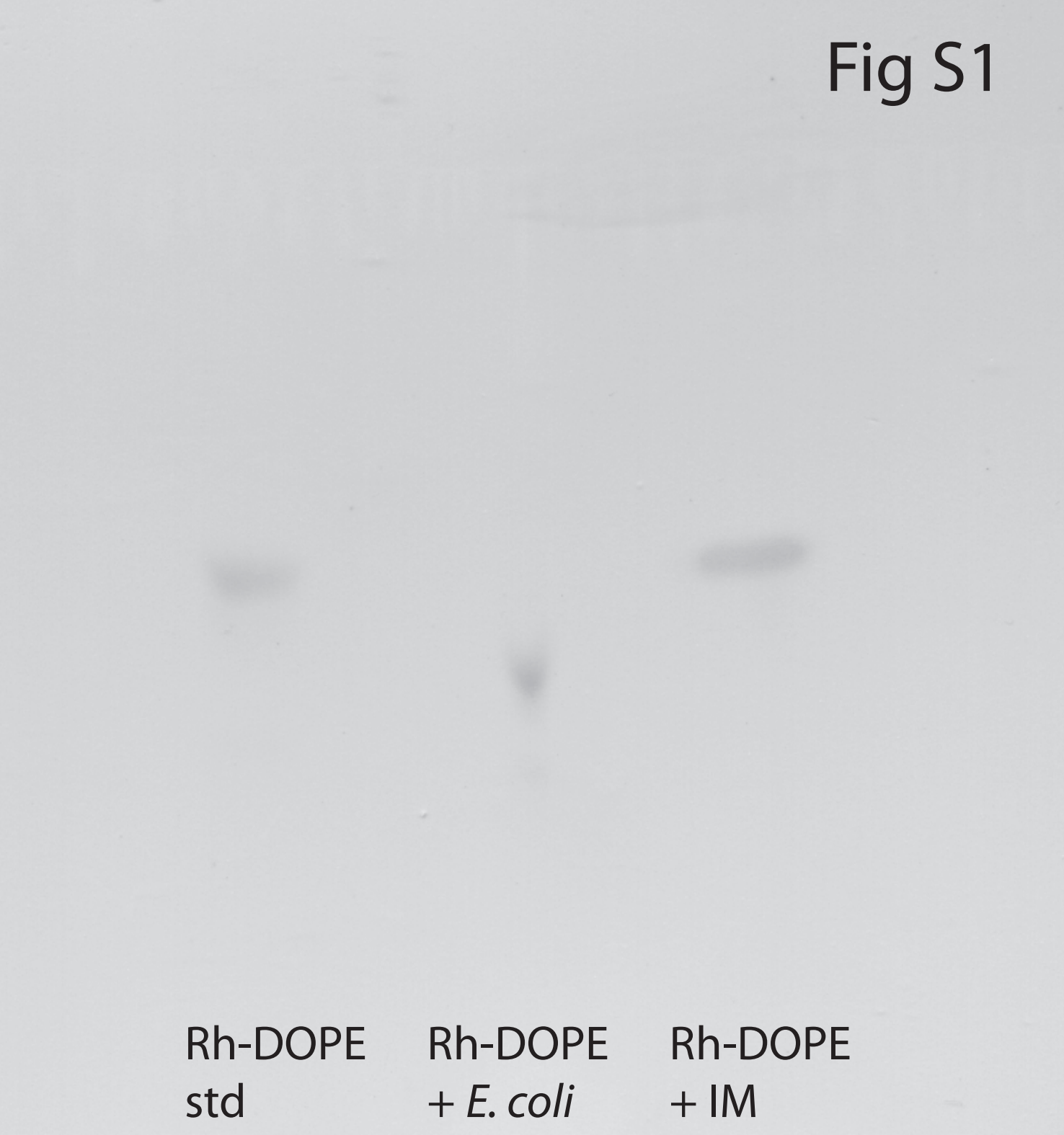

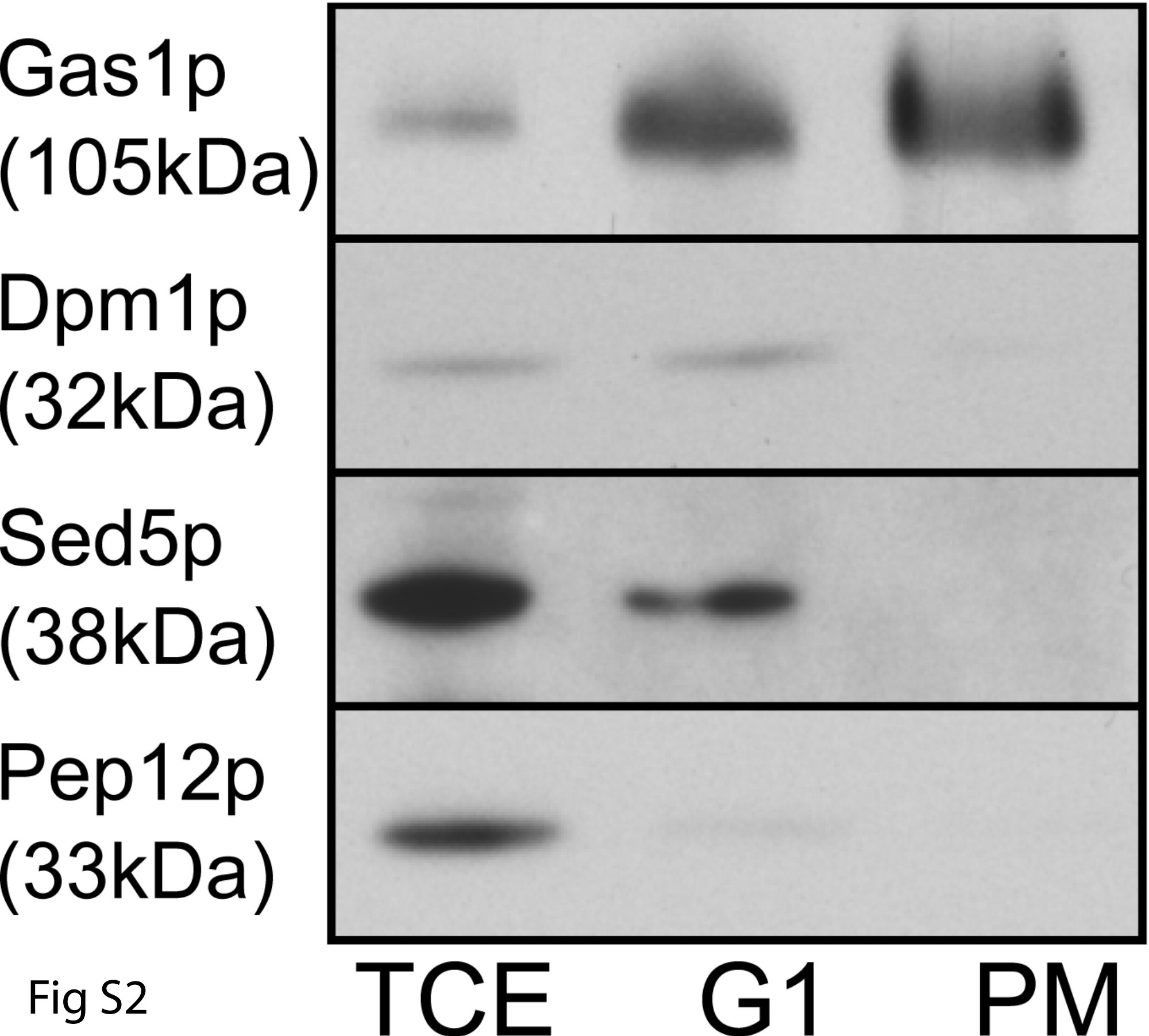

Fig S2

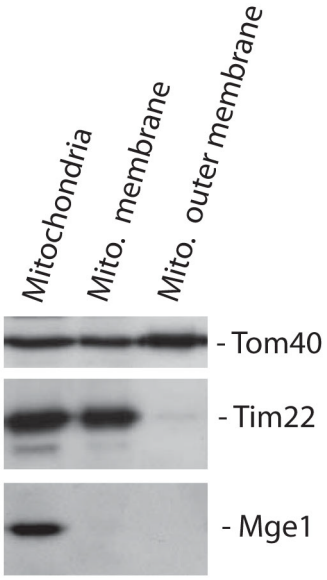

Fig S3

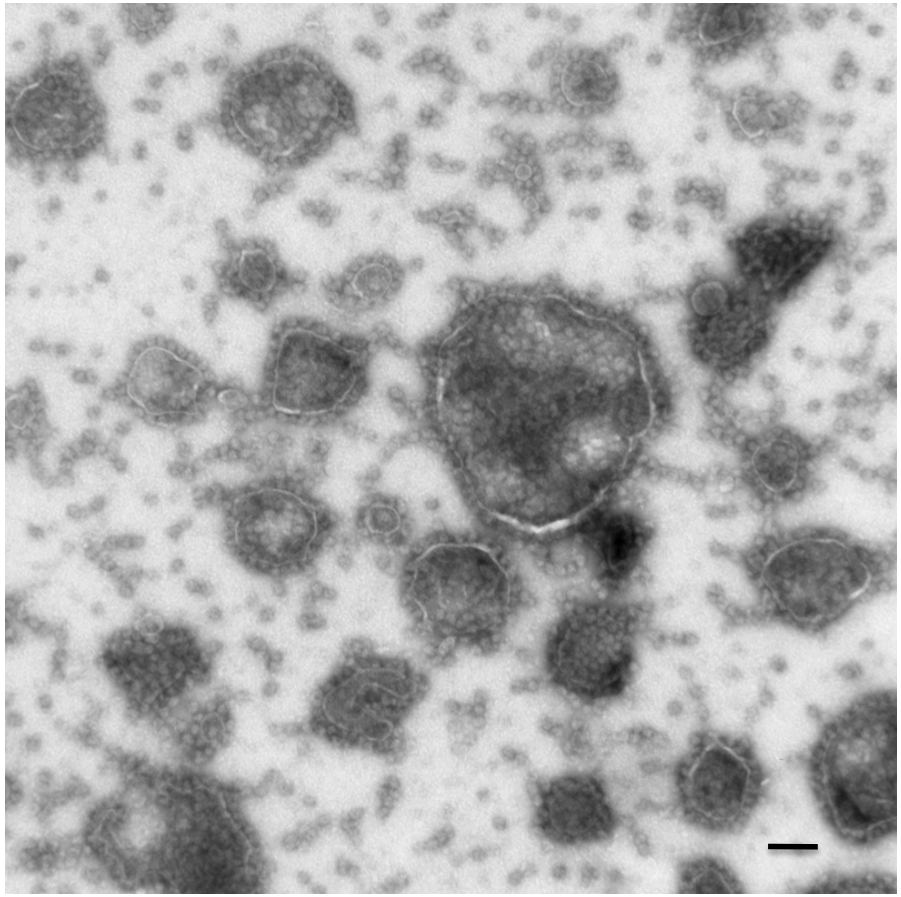

Fig. S4

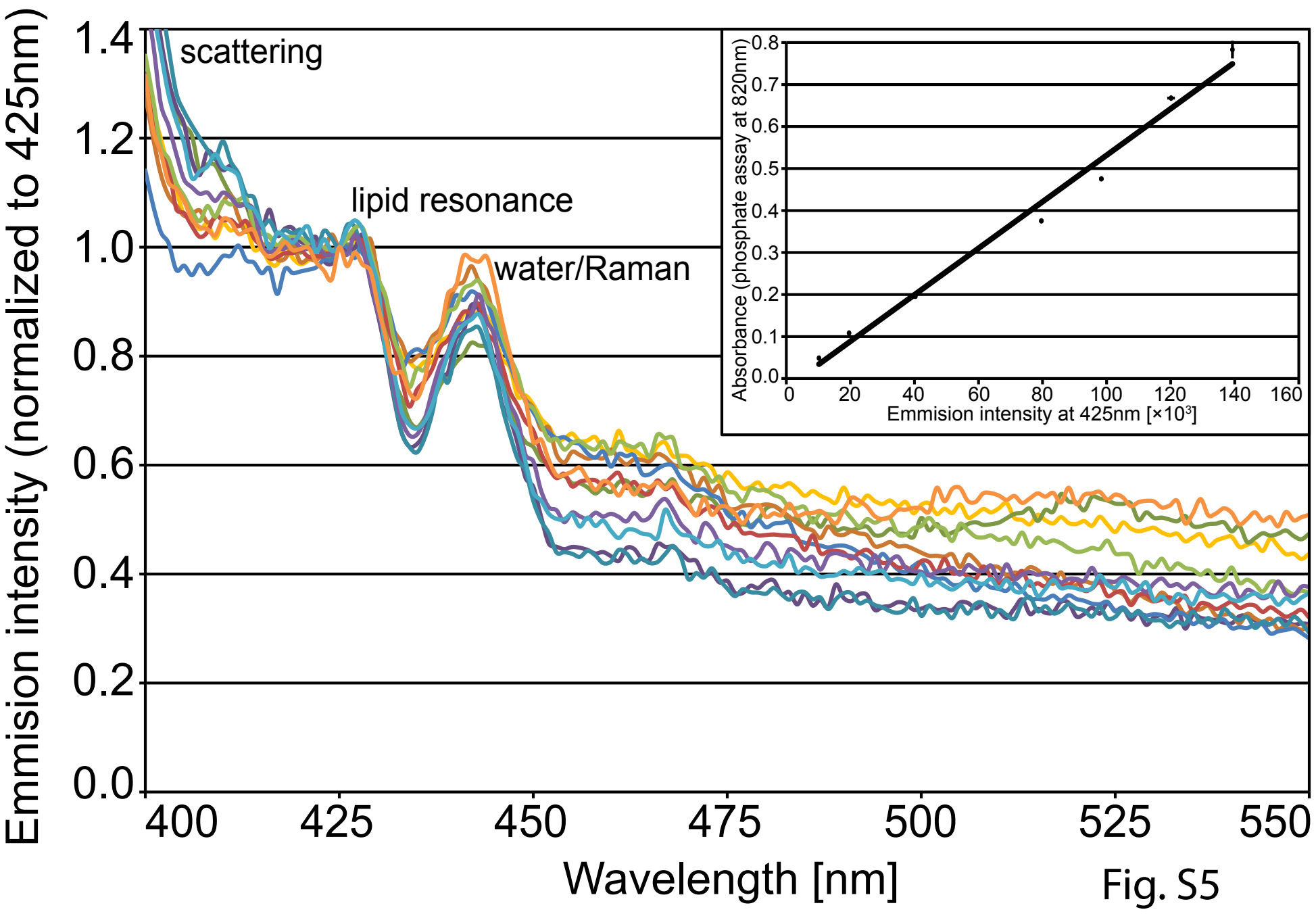
scattering
lipid resonance
water/Raman
Emmision intensity (normalized to 425nm)
Wavelength [nm]
1.4
1.2
1.0
0.8
0.6
0.4
0.2
0.0
400
425
450
475
500
525
550
Absorbance (phosphate assay at 820nm)
Emmision intensity at 425nm [×10³]
0.0
0.1
0.2
0.3
0.4
0.5
0.6
0.7
0.8
0
20
40
60
80
100
120
140
160

Fig. S5

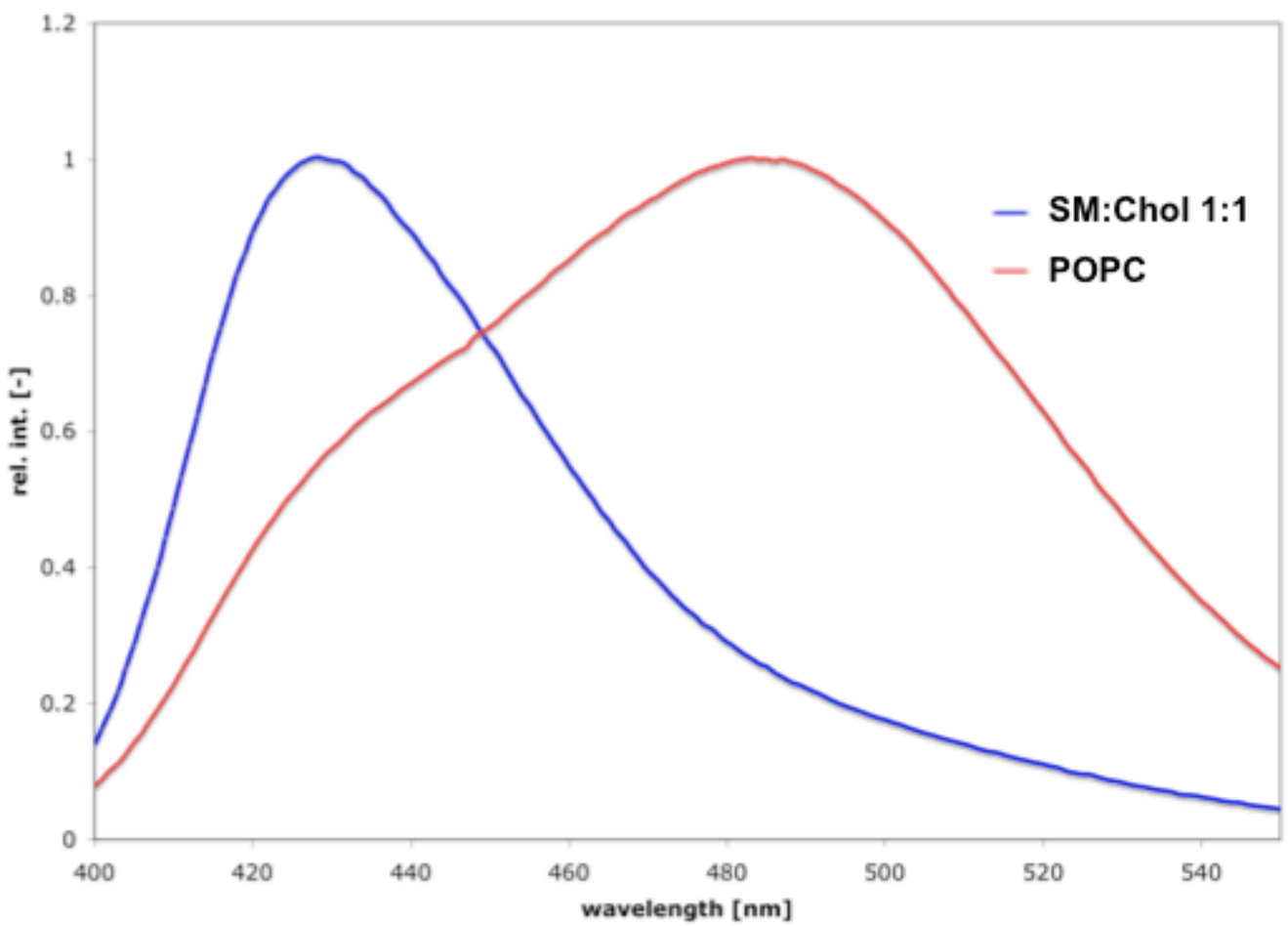

$$GP = \frac{\text{Intensity (400-460nm)} - \text{Intensity (470-530nm)}}{\text{Intensity (400-460nm)} + \text{Intensity (470-530nm)}}$$

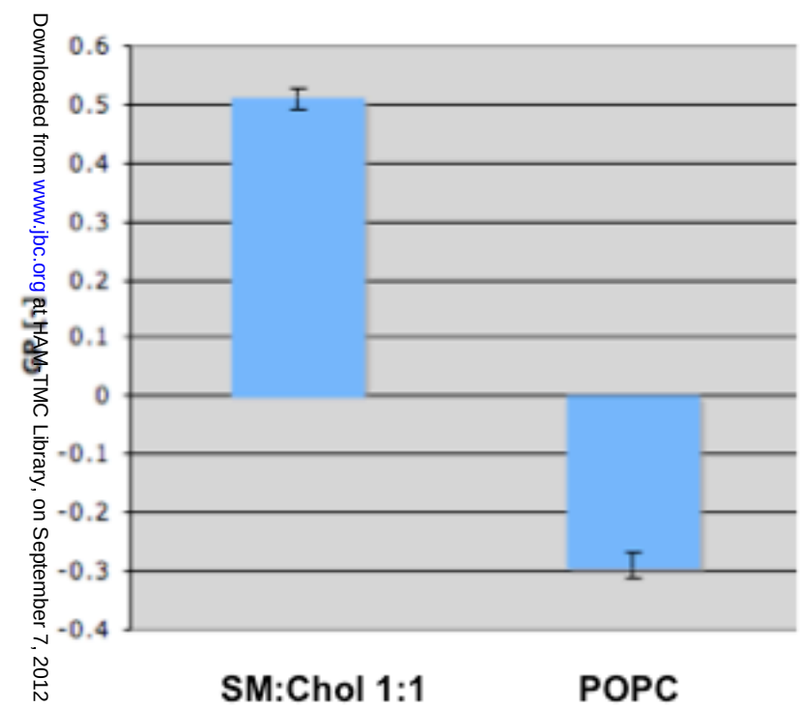

Fig. S6

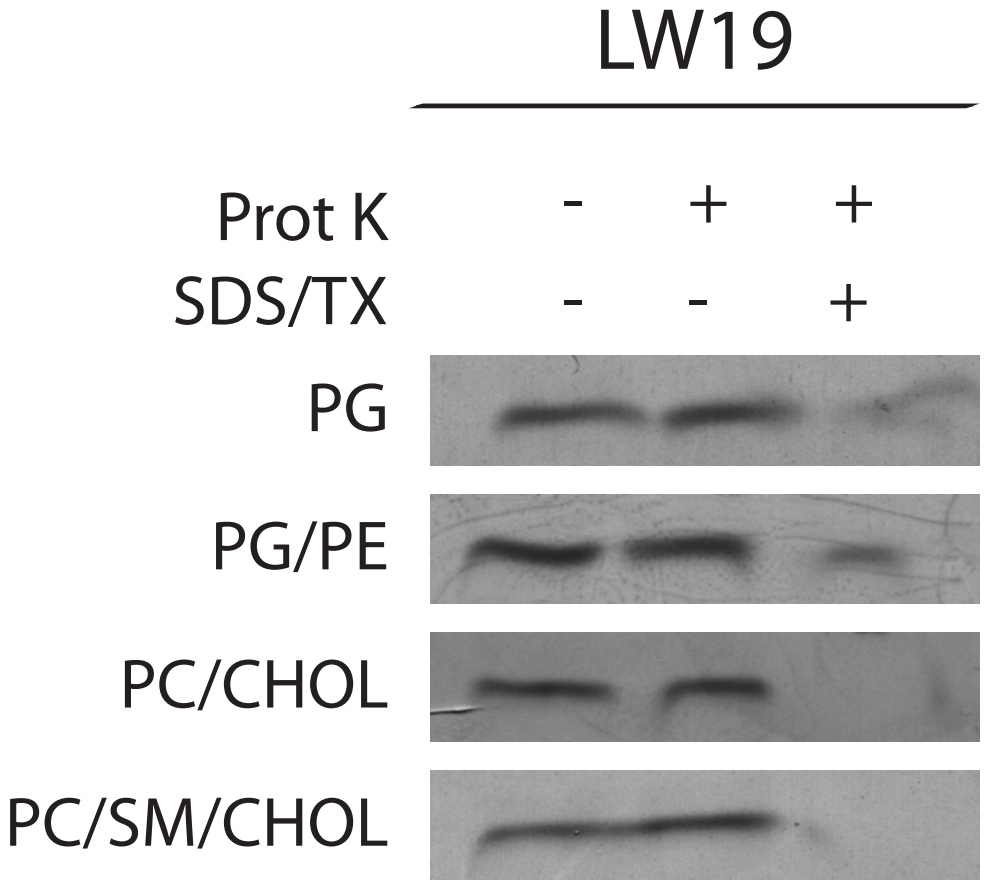

Fig. S7

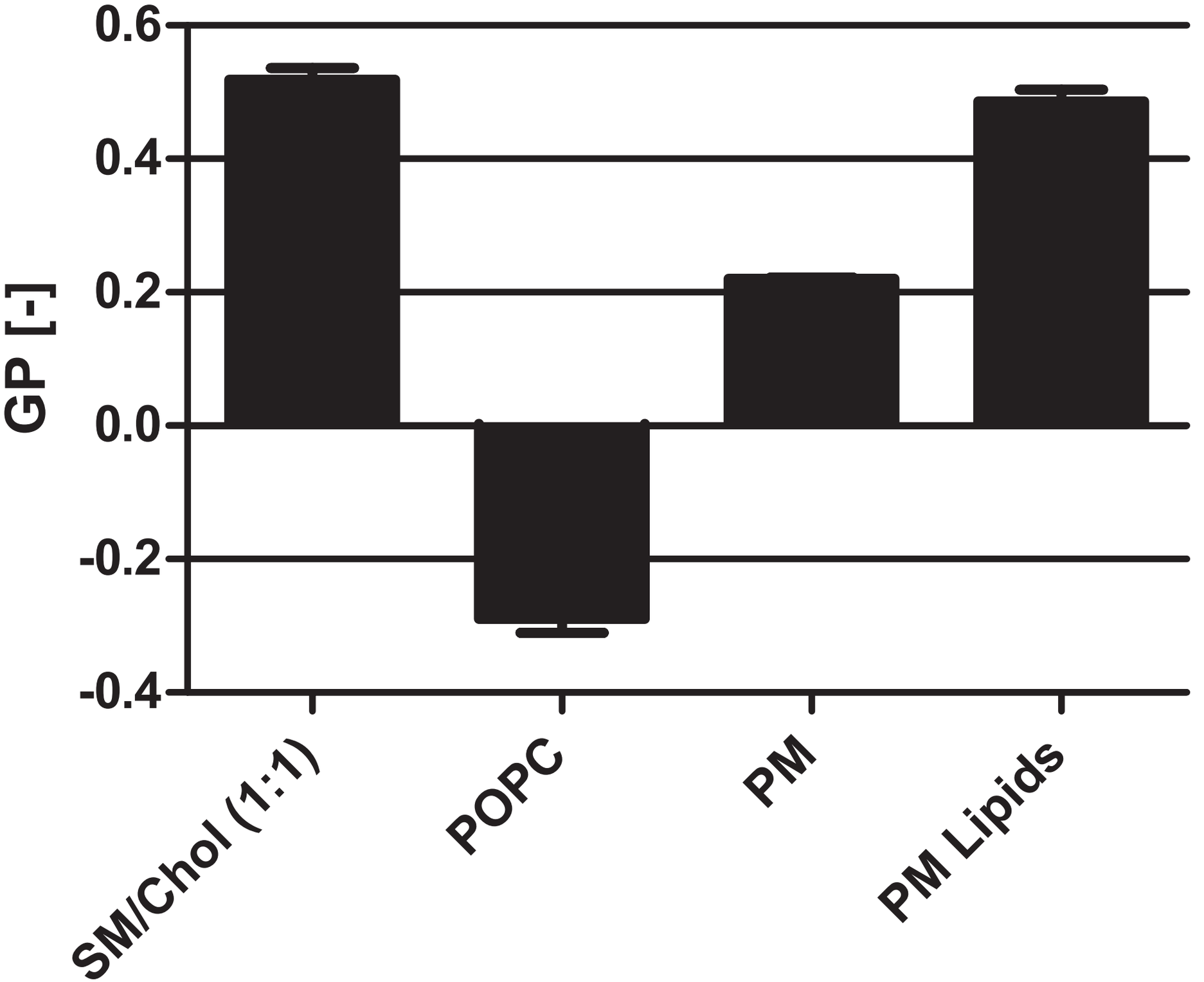

Fig. S8